Biobased ionic liquid solutions for an efficient post-combustion CO2 capture system

Carbon Capture Science & Technology 13 (2024) 100312

Contents lists available at ScienceDirect

Carbon Capture Science & Technology

journal homepage: www.elsevier.com/locate/ccst

Full Length Article

Biobased ionic liquid solutions for an efficient post-combustion CO_2 capture system

Salvatore F. Cannone [a,d,*], Michel Tawil [c,d], Sergio Bocchini [b,d], Massimo Santarelli [a,d]

[a] Department of Energy, Politecnico di Torino, Corso Duca degli Abruzzi 24, 10129 Torino, Italy
[b] Department of Applied Science and Technology, Politecnico di Torino, Corso Duca degli Abruzzi 24, 10129 Torino, Italy
[c] Department of Environment, Land and Infrastructure Engineering Politecnico di Torino, Corso Duca degli Abruzzi 24, 10129 Torino, Italy
[d] Centre for Sustainable Future Technologies CSFT@PoliTo Istituto Italiano di Tecnologia, Via Livorno 60, 10144 Torino, Italy

ARTICLE INFO

Keywords:
CO2 capture
Ionic liquid
Amino acid ionic liquid
Carbon dioxide

ABSTRACT

This study explores the use of ionic liquids (ILs) as a novel and efficient alternative to conventional monoethanolamine (MEA) for CO_2 capture. While MEA scrubbing is well-known for carbon sequestration, it faces limitations such as high energy consumption, toxicity, and rapid degradation. In contrast, ILs offer advantages such as non-volatility, stability, and reduced corrosiveness. We focus on a biodegradable IL comprising choline ([Cho]) and proline ([Pro]) amino acids to create an eco-friendly solution. Dimethyl sulfoxide (DMSO) is introduced as a diluent to mitigate viscosity issues during CO_2 uptake. Our research measures the thermo-physical properties, including density and viscosity of [Cho][Pro] in DMSO at different concentrations. The addition of DMSO resulted in a viscosity reduction of >97 % at a temperature of 303 K for the three virgin solutions compared to the pure IL. In addition, the CO_2 capture performance was evaluated using a system of absorption and desorption reactors. The results show that the 25 % wt [Cho][Pro] solution excels, achieving over 90 % CO_2 absorption, 0.66 mol_{CO_2}/mol_{IL} in the first cycle, and demonstrating high reusability and regeneration efficiency over multiple cycles. Comparisons indicate that the IL solution outperforms traditional aqueous MEA solutions. Longer term testing confirms the solution's stability and minimal degradation, achieving a regeneration efficiency of >55 % over 30 cycles, suggesting the potential of [Cho][Pro] for sustainable long-term CO_2 capture applications.

1. Introduction

Carbon capture, utilisation, and storage (CCUS) technologies enable the capture of CO_2 emissions from power plants, industrial processes, and biomass conversion, followed by their storage underground or utilisation for enhanced oil recovery and industrial applications. These technologies prevent CO_2 emission from contributing to the greenhouse effect and global warming [1,2].

Among the various CCUS processes, post-combustion capture (PCC) stands out for its broad applicability. PCC focuses on capturing CO_2 from flue gases emitted during fuel combustion in power plants, industries, and other sources. What makes PCC attractive is its potential to be retrofitted to existing plants with minimal modifications to the combustion process [3].

A specific approach within PCC is chemical absorption, where CO_2 undergoes a chemical reaction with solvent molecules. This process is particularly effective for capturing CO_2 from flue gas streams with relatively low concentrations. Chemical absorption processes offer advantages such as high CO_2 selectivity and high gas product purity [4].

Commonly used absorbents, such as amines like monoethanolamine (MEA), have drawbacks, including high corrosion rates, high water content in the purified gas outlet, high regeneration energy requirements often achieved through temperature increase, and significant evaporation losses. When using volatile absorbents, condensation from the purified gas stream or replenishment leads to higher operational costs. To address these limitations, researchers are improving the absorption medium by reducing volatility while maintaining high loading capacity [5].

Ionic liquids (ILs) have emerged as high promising candidates for the chemical capture of carbon dioxide. These unique materials consist of organic cations and inorganic or organic anions, which give these liquids exceptional properties such as low volatility, high thermal stability, and tunable solubility. The ability of ILs to chemically react with CO_2 makes them particularly attractive for CO_2 capture, offering advantages over traditional amine-based solvents [6].

One of the significant advantages of ILs in CO_2 capture is their low vapour pressure, eliminating concerns about solvent loss through evaporation. Additionally, ILs can be customized by modifying their chemical

* Corresponding author.
E-mail address: salvatore.cannone@polito.it (S.F. Cannone).

https://doi.org/10.1016/j.ccst.2024.100312
Received 27 June 2024; Received in revised form 15 September 2024; Accepted 19 September 2024

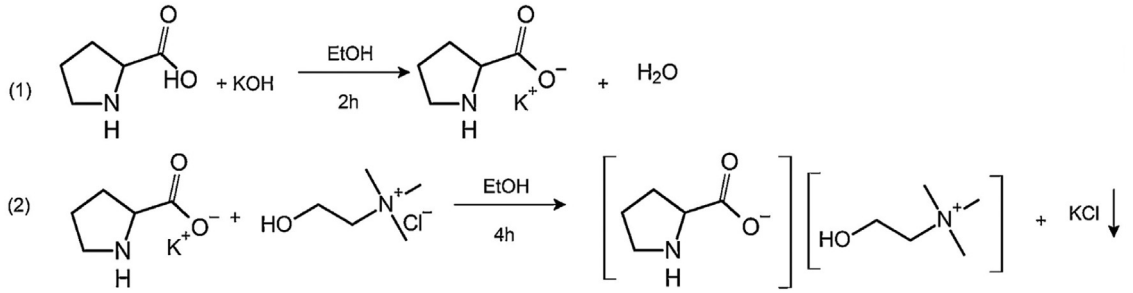

Fig. 1. Synthesis pathways of [Cho][Pro].

structure, enabling the design of ILs with improved properties, including higher CO_2 absorption capacity, lower toxicity, and increased stability. However, the implementation of ILs for CO_2 capture also faces challenges such as relatively high viscosity, which hinders the mass transfer rate of CO_2 and impacts the overall efficiency of the capture process. Researchers are actively exploring strategies to mitigate this issue by adding co-solvents or developing ILs with lower viscosity. Additionally, ongoing research and development efforts are focused on addressing the cost and scalability of ILs for large-scale CO_2 capture applications[7,8].

It is crucial to note that although ILs are considered 'green solvents,' the ILs commonly studied for CO_2 capture predominantly use imidazolium and pyridinium cations paired with fluorinated anions, posing challenges for biodegradability and biocompatibility. Thus, from an environmentally conscious standpoint, it is essential to prioritize the selection of non-toxic and biocompatible cations/anions as a crucial step in the development of a sustainable CO_2 capture process utilising ILs [9].

In our previous studies, we investigated the use of biodegradable functionalized ionic liquids (ILs) composed of environmentally friendly metabolic molecules, such as choline [Cho] and various amino acid [AA] anions, including glycine, alanine, serine, and proline. To address the issue of increased IL viscosity during CO_2 absorption, we employed dimethyl sulfoxide (DMSO) as a diluent for the [Cho][AA] IL. DMSO provides several advantages, such as inhibiting carbonate formation, having a high boiling point, being non-toxic, and being completely miscible with the IL. Literature indicates that DMSO shows low solubility for CO_2 at low pressures, while it effectively absorbs H_2S [10,11]. This property can be beneficial in a multi-step gas purification process, where DMSO is used for H2S removal before CO_2 capture. Testing ionic liquids diluted in DMSO, we have observed the formation of carbamic acid (mechanism 1:1) and ammonium-carbamate (mechanism 2:1) during the interaction of CO_2 with amino acids, resulting in a molar efficiency exceeding 0.5 mol CO_2/mol amine, a characteristic typical of primary amines like MEA [12].

Furthermore, we conducted measurements of the thermophysical properties, including density and viscosity, of the selected solutions. These measurements were carried out with pure ionic liquid and solutions composed of 12.5wt % [Cho][AA] in DMSO. The results demonstrated a significant reduction in viscosity by approximately three orders of magnitude and a slight decrease in density, approaching values similar to the solvent [13]. Gravimetric measurements were employed, assessing CO_2 absorption capacity and the performance of multiple absorption/desorption cycles. Comparative tests involving different [Cho][AAs] and various dilutions in DMSO revealed that: (i) [Cho][Phe] possess the lowest absorption capacity at any concentration; (ii) [Cho][Gly] and [Cho][Ala] produce solid participate during CO_2 capture process; (iii) [Cho][Ser] exhibits the lowest CO_2 loading value and medium stability; (iv) [Cho][Sar] instead is the most performing IL but their performance suddenly decrease. Therefore, the [Cho][Pro] solution, containing a heterocyclic moiety with a secondary amine, which exhibited the highest stability throughout the absorption cycles and demonstrated superior CO_2 absorption capacity compared to other tested solutions was chosen to be investigated in this work [14].

The primary objective of this study is to gain valuable insights into the absorption and desorption performance of [Cho][Pro] in DMSO across varying concentrations (12.5 % wt, 25 % wt, and 50 % wt). By systematically exploring different concentrations, we aimed to determine the specific concentration that exhibits the most promising and favourable performance characteristics.

To achieve this objective, density and viscosity measurements were conducted across a temperature range of 25 °C to 70 °C to evaluate the performance of various solutions with different ionic liquid fractions in DMSO. The absorption and desorption tests were carried out using a scale-up test rig, consisting of two stainless steel-packed columns. This test rig was equipped with an electrical heating system, fluid recirculation system, gas analyser, and multiple temperature and pressure sensors to comprehensively evaluate the CO_2 capture performance of the IL. The influence of temperature on the absorption step was thoroughly investigated. Furthermore, a long-duration test was conducted to assess the stability of the IL, the resulting samples were analyzed using ATR-infrared spectrometry.

2. Materials and methods

2.1. Material synthesis

In a typical synthesis, 56.2 g of potassium hydroxide pellets (purity ≥85 %, supplier: Carlo Erba) were dissolved in 300 ml of methanol (purity ≥99.8 %, supplier: Merck) under stirring. Then, 57.57 g of l-proline (purity ≥99 %, supplier: Merck) was added to the solution. As a result, a white suspension with the formation of some precipitate was observed, indicating the formation of the potassium salt of proline; the excess potassium salt precipitates. After 2 h of continuous stirring, the complete dissolution of potassium hydroxide pellets was achieved. Thus 69.81 g of choline chloride (purity ≥98 %, supplier: Alfa Aesar) were added. The solution was stirred for 4 h to ensure the complete dissolution of the potassium salt of proline, the formation and precipitation of potassium chloride, and the formation of choline proline in the solution. The resulting mixture was centrifugated to separate the potassium chloride crystals formed, the precipitate was washed with methanol to recover the adsorbed ILs. The initial solution containing the IL and the methanol recovered were combined and subjected to solvent evaporation. To eliminate any remaining traces of methanol and water, subject the obtained [Cho][Pro] ionic liquid to overnight outgassing under a dynamic vacuum at 30 °C. The reactions describing the whole synthetic process are summarized in Fig. 1.

[Cho][Pro] was diluted in dimethyl sulfoxide (DMSO, supplied by Merck, purity ≥99 %) To address the issue of increased viscosity during CO_2 absorption, DMSO is used as a diluent. Dilutions in DMSO were performed to reach 12.5 %, 25 % and 50 % wt concentrations.

2.2. Characterization

Density assessments of the pure [Cho][Pro] ionic liquid and its varying concentrations in DMSO were conducted using a Gay-Lussac pyc-

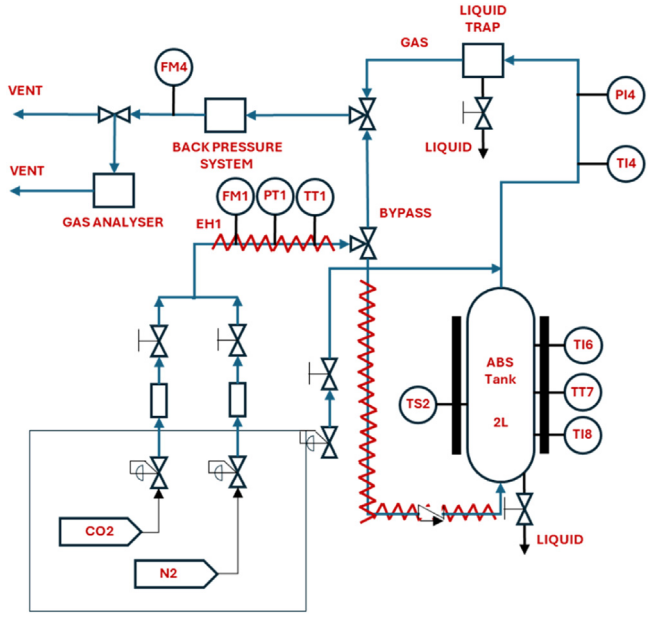

Fig. 2. Scheme plant of the test bench.

nometer across a temperature spectrum from 25 °C to 70 °C. This instrument, a glass flask featuring a capillary stopper, facilitated the precise density measurement. A comprehensive methodology is detailed in Chapter 1 of the supplementary materials. The study further extended to evaluating the kinematic viscosities of the undiluted [Cho][Pro] and its solutions by employing a Cannon-Fenske viscometer, adhering to the stringent guidelines of the ASTM D445 and D446 standards. To ascertain the dynamic viscosity, the previously obtained kinematic viscosity values were normalized by the respective density measurements. This protocol is detailed in Chapter 2 of the supplementary material.

Characterization of the 25 % [Cho][Pro] in DMSO solution post-stability analysis was conducted through Attenuated Total Reflection Infrared Spectroscopy (ATR-IR), utilizing a Bruker Invenio R Fourier Transform Spectrophotometer outfitted with a mercury-cadmium-telluride (MCT) cryogenic detector. Spectral data were compiled by amassing 32 scans (and 64 scans for background spectra) across the wavenumber range of 4000 to 600 cm^{-1}, achieved with a 2 cm^{-1} resolution.

2.3. Absorption and regeneration measurement of CO_2

The experimental setup for evaluating the performance of the solutions, depicted in Fig. 2 SM 2 of the supplementary material, mirrors the dual-column arrangement widely adopted in large-scale carbon capture facilities. For this initial work, only part of the experimental rig described in the supplementary material was used, as shown in Fig. 2. This system comprises one stainless steel packed column with a 2-litre capacity. The gas flow mixture control is achieved using Mass Flow Controllers (MFCs – Brooks Instrument, USA), with mass flow meters strategically positioned at the absorption column's inlet and the outlets of the column. A back pressure control mechanism ensures the preservation of the desired pressure levels within the column.

Temperature regulation is crucial for the optimal functioning of the experimental test rig. Therefore, a heating apparatus using electrical resistors is employed to keep the gas and solvent temperatures within the target range. The setup is further enhanced with temperature, pressure, and flow sensors, enabling precise monitoring of these variables throughout the experiment.

A mass spectrometer from Hyden Analytical is integrated into the system to assess the carbon capture process's efficacy. This instrument offers accurate assessments of the flue gas composition before and after carbon capture, shedding light on the absorption and desorption phases effectiveness.

2.4. Theory

All tests were conducted feeding pure CO_2 during absorption phase. The difference in volume flow rate between the inlet and outlet sides of the column was measured using two calibrated flow meters to quantify the amount of CO_2 captured during the absorption tests. A preliminary 3-cycle desorption test was performed on the 50wt % solution of [Cho][Pro]. The test aims to verify the desorption capacity of the solution thermally, in an anhydrous environment, and at low partial pressure of CO_2 by insufflating nitrogen (N_2) into the column. The results described in the supplementary material show that the regeneration of the material at the set desorption temperature alone, or in anhydrous environment are only partial, and that therefore regeneration needs to operate at lower CO_2 partial pressures (through the installation of a vacuum pump, or by means of a gas sweep). Therefore, in the desorption phase a steady stream of N_2 enters and exits the regeneration column at a fixed flow rate. The outlet gas, composed of inlet N_2 and desorbed CO_2, was analysed continuously to determine the amount of desorbed CO_2, according to [1. In this equation, $V_{CO_2,out}$ represents the volume flow rate of the CO_2 desorbed, $V_{N_2,in}$ is the volume flow rate of nitrogen at the inlet section and $x_{N_2,out}$ is the concentration of N_2 at the outlet of the reactor. Both the volume flow rates are expressed in $[Nl/h]$.

$$V_{CO_2,out} = \frac{V_{N_2,in}}{x_{N_2,out}} \tag{1}$$

CO_2 absorption loading refers to the amount of CO_2 captured and retained by a particular absorbent material or solvent. It is a crucial parameter in carbon capture processes, where the goal is to selectively remove CO_2 from flue gases or other emission sources. The absorption loading capacity is typically expressed as the mass of CO_2 absorbed per unit mass of the solution composed of solvent and IL (i.e., see [2), while the molar efficiency, expressed in [3, represents the mole of absorbed CO_2 per mole of ionic liquid. They represent the maximum amount of CO_2 that can be captured and retained under specific operating conditions, such as temperature, pressure, and concentration of CO_2 in the gas stream.

$$m = \frac{m_{CO_2}}{m_{solution}} \tag{2}$$

$$\alpha = \frac{n_{CO_2}}{n_{IL}} \tag{3}$$

The CO_2 removal rate refers to the rate at which CO_2 is removed from a gas stream. It is a measure of how effectively a carbon capture process can reduce the concentration of CO_2 in a specific system and it is typically expressed as the amount of CO_2 removed per unit of time ($m_{CO_2,abs}$) divided per the quantity of CO_2 that enters into the column ($m_{CO_2,in}$).

$$\psi = \frac{m_{CO_2,abs}}{m_{CO_2,in}}\% \tag{4}$$

The CO_2 removal rate depends on several factors, including the design and efficiency of the capture technology, the properties of the solution material used, the flow rate of the gas stream, and the concentration of CO_2 in the feed gas. Higher removal rates are desirable for efficient carbon capture systems as they indicate a faster and more effective reduction in CO_2 levels.

In carbon capture processes, absorbents or adsorbents capture CO_2 from a gas stream, and after reaching their capacity, they undergo a regeneration step to release the captured CO_2 and restore their adsorption capacity. The regeneration efficiency, in this context, quantifies the

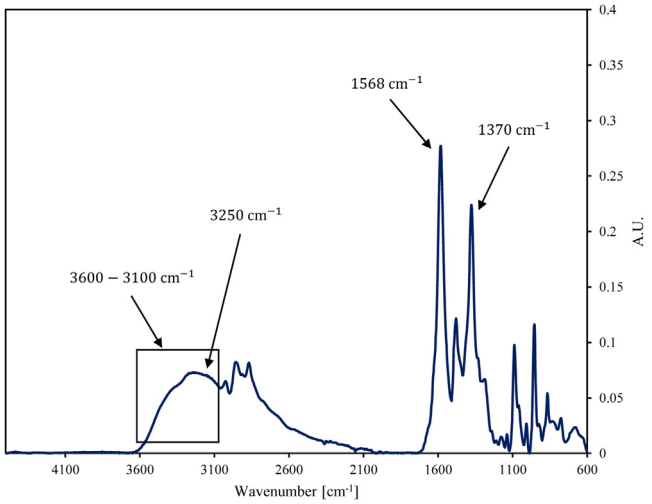

Fig. 3. Vibrational frequencies for carboxylate (1568 and 1370 cm^{-1}), asymmetric stretching of the amine group (~3250 cm^{-1}) and stretching of cholinate hydroxile at 3600–3100 cm^{-1}.

ability of the regeneration process to recover CO_2 for reuse. To calculate the regeneration efficiency, one must compare the amount of CO_2 captured in a particular cycle (n-th cycle) to the amount captured in the first cycle. The higher the regeneration efficiency, the greater the fraction of CO_2 that can be successfully recovered. A higher efficiency indicates a more effective regeneration process, reducing the need for additional CO_2 capture materials and potentially improving the overall economic viability and environmental sustainability of carbon capture technologies.

$$\eta = \frac{m_n}{m_1}\% \tag{5}$$

It's important to note that regeneration efficiency can be influenced by various factors, including the specific regeneration conditions, the properties of the absorbent or adsorbent material, and the overall design and operation of the carbon capture system.

3. Results and discussion

3.1. Chemical characterization of [Cho][Pro]

The assessment of [Cho][Pro] synthesis was conducted using ATR infrared spectroscopy, yielding the following observations: as anticipated, the ammonium-related bands, as identified by bending (δ) of zwitterionic NH_2^+ at 1550 cm^{-1} [14] in pure proline, disappears in neutral amine signals in the [Cho][Pro] spectrum, while the carboxylate stretching signals remain largely unaffected across all compounds. The [Cho][Pro] spectrum, shown in Fig. 3, integrates the spectral characteristics of both Proline and choline chloride. Notably, the distinct OH stretching peak of choline chloride is transformed in the ionic liquid, resulting in a broad band spanning 3600–3100 cm^{-1}. This band overlaps with the amine and ammonium stretching modes, indicative of the interaction between the choline OH group and the amino acid entities. Furthermore, the vibrational frequencies associated with carboxylate are observed at 1568 and 1370 cm^{-1}, and the asymmetric stretching of the amine group is noted around 3250 cm^{-1}, corroborating findings previously reported [14].

3.2. Density and viscosity of [Cho][Pro]

Density measurements were conducted at ambient pressure and between 20 °C and 70 °C. However, for solutions with 50 % wt [Cho][Pro] in DMSO and pure [Cho][Pro], it was not possible to perform measurements at the full range of temperatures. This limitation was due to the extremely high viscosity of these liquids at lower temperatures, which made accurate density measurements challenging despite careful calibration. The results of the density measurements are presented in Fig. 4. The data points exhibit a strong linear relationship, indicating a direct inverse correlation between density and temperature. The empirical [6 is derived based on this linear dependence. The values of the fitting coefficients A_1 and A_2, as well as the correlation coefficients R^2 and the standard deviations *SDS*, are provided in Table 1.

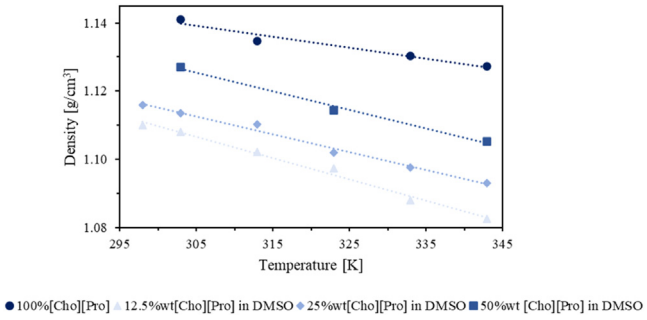

Fig. 4. Density ρ as a function of temperature.

Table 1
The fitting parameters A_1 and A_2, standard deviations (SDs), and the coefficient of determination (R^2) for the empirical equations describing the density as a function of temperature are provided for the solutions at different concentrations considered.

Solution	A_1	A_2	SD	R^2
100 %wt [Cho][Pro]	−0.0003	1.2364	0.006	0.953
12.5 %wt [Cho][Pro] in DMSO	−0.0005	1.2915	0.034	0.989
25 %wt [Cho][Pro] in DMSO	−0.0005	1.2727	0.008	0.987
50 %wt [Cho][Pro] in DMSO	−0.0006	1.2978	0.012	0.990

Table 2
Fitting parameters A_3 and A_4, SDs and R^2 of the obtained empirical equations of viscosity as functions of temperature for the solutions at varying concentrations considered.

Solution	A_3	A_4	SD	R^2
100 %wt [Cho][Pro]	2.00E+08	−0.062	1.99E-01	0.998
12.5 %wt [Cho][Pro] in DMSO	0.7155	−0.018	5.15E-05	0.999
25 %wt [Cho][Pro] in DMSO	3.966	−0.022	4.20E-04	0.998
50 %wt [Cho][Pro] in DMSO	325.3	−0.032	2.30E-03	0.999

$$\rho(T) = A_1 \cdot T + A_2 \tag{6}$$

Consistent with expectations, an overall decreasing trend in density is observed with increasing temperature for all three solutions at various concentrations. The correlation coefficients for these solutions exceed 0.98, indicating a high degree of linearity in the relationship between density and temperature. Additionally, the data reveals that density increases with higher concentrations of [Cho][Pro], which can be attributed to the significantly greater molecular weight of [Cho][Pro] (219.3 g mol^{-1}) compared to DMSO (78.13 g mol^{-1}). The experimental viscosity data, presented in Fig. 5, exhibit an exponential trend that aligns well with the empirical [7. The fitting coefficients A_3 and A_4, along with the standard deviations (SDs) and correlation coefficients (R^2), are provided in Table 2.

$$\mu(T) = A_3 \cdot e^{A_4 \cdot T} \tag{7}$$

Consistent with expectations, the viscosity values decrease as the temperature increases. The correlation coefficient surpasses 0.99 for all the solutions studied.

Notably, significant differences in viscosity are observed between the pure [Cho][Pro] and the other solutions, with variations spanning three orders of magnitude, particularly evident in the 12.5 % weight solution.

Table 3
Quantity of solution loaded into the reactor.

Solution	Mass of solution in reactor [kg]	Mass of reagent in reactor [g]	Mole of reagent in reactor [mol]
12.5 %wt [Cho][Pro] in DMSO	0.55	68.65	0.31
25 %wt [Cho][Pro] in DMSO	1.0	249.78	1.14
50 %wt [Cho][Pro] in DMSO	1.03	516.05	2.35
30 %wt MEA in water	0.41	122.1	2.0

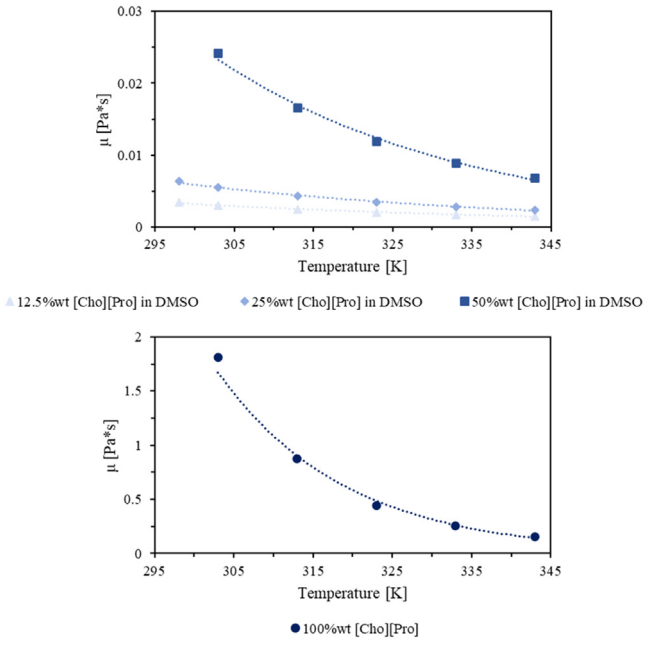

Fig. 5. Dynamic viscosity μ as a function of temperature.

The findings underscore the critical role of solvent dilution in carbon capture endeavours and highlight the need for refining mass transfer processes when employing Ionic Liquids (ILs) for enhanced efficiency.

3.3. Absorption and desorption tests

In order to investigate the absorption and desorption processes independently, a batch configuration is employed in the experimental setup, utilising the single absorption column. The experiments are conducted at ambient pressure with a constant specific flow rate of 30 $\frac{Nl}{h}/mol_{IL}$ for both absorption and desorption operations. The inlet streams are intentionally composed of pure CO_2 flows, facilitating the assessment of both chemical and physical absorption phenomena to isolate the effects of carbon capture and release. To facilitate a direct comparison between the performance of the [Cho][Pro] IL absorbent and a commonly used industrial absorbent, monoethanolamine (MEA), we conducted additional experiments using a solution composed of 30 % wt MEA in water. Three different solutions at different [Cho][Pro] compositions are used, while the MEA solution was involved to compare the absorption/desorption processes of the three proposed solutions with the state of the art under the same operating conditions and reactor. Table 3 reports the material data.

3.3.1. Cyclability performance

Two tests were conducted to evaluate the absorption performance and regeneration efficiency of the three solutions at different compositions. The first set of tests involves a sequence of three consecutive cycles: 90 min of absorption, 90 min of desorption, and cooling at ambient temperature. The absorption stage begins at an initial temperature of 30 °C, while the desorption stage starts at the temperature of the end of the absorption process and then rises to 80 °C. This series of tests aims to determine the absorption capacity of the fresh solution as well as the regeneration efficiencies achieved after each cycle and compare the performance of the 3 innovative solutions with those obtained with a solution composed of 30 % MEA in water used as a benchmark. Table 4 summarises the operating conditions of the cyclability test. For each solution, the inlet flow rate increases from 9 to 34 to 71 Nl/h for the 12.5 %, 25 %, and 50 % [Cho][Pro] solutions, respectively, and 60 Nl/h for benchmark solution: this adjustment was made to achieve a CO_2 flow rate to IL molar ratio constant at $30\frac{\frac{Nl_{CO2}}{h}}{mol_{IL}}$. This design ensures that the CO_2 loading per mol of IL is consistent across all tests, allowing for a direct comparison of the CO_2 absorption performance at different IL concentrations under controlled conditions.

The main part of the discussion presents aggregated data that allow for a comparison between the different solutions. Individual graphs obtained from each test performed (see Figure SM4, SM5, SM6 and SM7), including CO_2 loading, CO_2 desorbed flow rate, and temperature evolution inside the column, are provided in the supplementary material. These detailed graphs offer a more comprehensive view of the experimental results. The results presented in Fig. 6 demonstrate the molar absorption loading evolution during three sequential cycles of absorption and desorption for different solution compositions. The 12.5 % wt [Cho][Pro] in DMSO solution consistently exhibits higher absorption

Table 4
Operating conditions of the cyclability test.

Solution	condition	T [°C]	P [bar]	Flow composition [%]	Flow rate [Nl/h]
12.5 %	Absorption	30	1	100 % CO_2	9
	Desorption	80	1	100 % N_2	9
	Cooling	T_{env}	1	–	–
25 %	Absorption	30	1	100 % CO_2	34
	Desorption	80	1	100 % N_2	34
	Cooling	T_{env}	1	–	–
50 %	Absorption	30	1	100 % CO_2	71
	Desorption	80	1	100 % N_2	71
	Cooling	T_{env}	1	–	–
30 % MEA	Absorption	30	1	100 % CO_2	60
	Desorption	80	1	100 % N_2	60
	Cooling	T_{env}	1	–	–

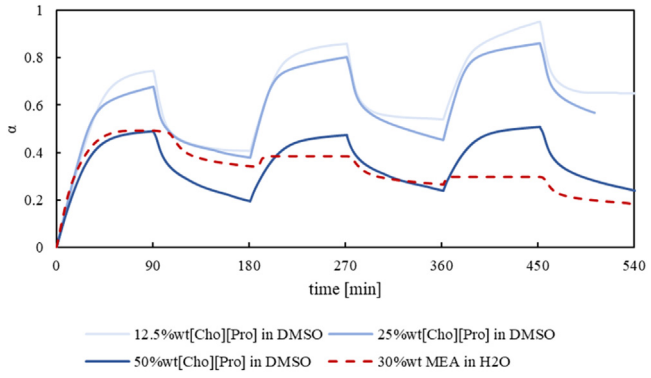

Fig. 6. Absorption/desorption cyclability test.

loading, reaching values of 0.74, 0.85, and 0.95 mol_{CO_2}/mol_{IL} in the first, second and third cycle, respectively. On the other hand, the solution with 50 % wt [Cho][Pro] in DMSO, which has a higher IL concentration, fails to surpass the theoretical limit observed with primary amines (i.e., the CO_2 uptake of primary and secondary amine solutions is driven by the zwitterion reaction mechanism that shows the theoretical limit of 0.5 mol_{CO_2}/mol_{amine} [15]), exhibiting molar absorption loading below 0.5 mol_{CO_2}/mol_{IL} in each cycle. The theoretical limit reported in the literature was further validated using our experimental setup. Fig. 6 shows the test conducted on the commercial MEA solution under the same operating conditions as the ionic liquid solutions. During the first absorption cycle, the MEA solution reached the theoretical limit of 0.5 mol CO_2/mol MEA. As anticipated from the literature, the operating conditions used in the regeneration step were not optimal for this solution. Typically, CO_2 stripping is performed by introducing water vapor at around 100–120 °C [16]. However, in our setup, regeneration was carried out at 80 °C using nitrogen, which was insufficient to fully remove the absorbed CO_2. Although this work did not include a detailed study of the heat of reaction, this initial comparison suggests that the energy required to remove CO_2 from the ionic liquid solutions is lower than that needed for the reference solution. The observed trend obtained from ionic liquid solutions can be further explained by considering the findings from [17], which describe the CO_2 absorption mechanisms in choline-amino acid ionic liquids (AAILs) using operando ATR-IR spectroscopy. Specifically, the study highlights that the interaction of CO_2 with [Cho][Pro] in DMSO involves the formation of carbamic acid and ammonium-carbamate species, with the formation mechanisms and the extent of these species being influenced by the concentration and composition of the IL solution. The higher absorption loading in the 12.5 % wt solution suggests that at lower IL concentrations, the ionic liquid molecules are more effectively dispersed, facilitating the absorption of CO_2 through both the formation of carbamic acid and the cooperative interaction mechanisms described in Latini et al. [17]. Additionally, as supported by the study on the CO_2 absorption capacities of similar choline-based ILs, the absorption capacity of these ILs is significantly influenced by the solubility and dispersion of the IL in the solvent [17]. This is consistent with the reduced performance observed in the 50 % wt [Cho][Pro] in DMSO solution, where the higher viscosity and potential aggregation of IL molecules likely hinder the effective absorption of CO_2. These findings align with the theoretical predictions and experimental data indicating that the optimal performance of CO_2 capture with ILs often occurs at specific concentration ranges where the IL molecules are sufficiently mobile and dispersed to interact with CO_2 effectively. This finding has also been reported by other researchers in the literature. For example, Hu et al. investigated the effect of water concentration (0 % to 40 %) in the ionic liquid solution [18]. They found that CO_2 absorption capacity increases with increasing water content. These results suggested that the presence of water in ILs promotes CO_2 absorption and one of the reasons for this have been explained showing that water reduces the viscosity of ILs, further indicating that the viscosity of the IL plays a role in CO_2 absorption capacity. The 25 % wt [Cho][Pro] mixture demonstrates intermediate performance, closer to the lowest concentration solution, with molar absorption loading values progressively reaching 0.68, 0.8 and 0.86 mol_{CO_2}/mol_{IL}.

Under the given regeneration conditions, complete removal of absorbed CO_2 in each cycle is not achievable for any of the three solutions at the operating conditions. Particularly, the first regeneration process results in <50 % CO_2 desorption for the 12.5 % and 25 % wt [Cho][Pro] solutions, while the solution with 50 % wt IL desorbs 60 % of the initially absorbed CO_2. However, in subsequent cycles, all solutions demonstrate the ability to desorb >70 % of the newly absorbed CO_2, as summarized in Table 5. The potential for reaching a steady-state condition where all newly absorbed CO_2 will be subsequently desorbed during regeneration was evaluated in the long-term stability test.

As reported in Fig. 7 (left axis), the mass of CO_2 absorbed consistently decreases as the solutions become more diluted. In the first cycle, approximately 49 $g_{CO_2}/kg_{solution}$, 34 $g_{CO_2}/kg_{solution}$, and 19 $g_{CO_2}/kg_{solution}$ are absorbed from the 50 % wt, 25 % wt and 12.5 % wt [Cho][Pro] solutions, respectively. In contrast, the benchmark solution demonstrated significantly superior performance in this regard, achieving 108.5 $g_{CO_2}/kg_{solution}$,. This marked difference in the first absorption step is attributed to the lower molar mass of MEA (61.1 g mol^{-1}) compared to the 219.3 g mol^{-1} of the Choline Proline molecule. In subsequent cycles, the difference in mass CO_2 absorption loading between the 50 % wt IL solution and the others diminishes. The difference between one cycle and the next is halved, from 15 to 6.8 $g_{CO_2}/kg_{solution}$ for the intermediate solution, and from 30 to 17 $g_{CO_2}/kg_{solution}$ for the less concentrated solution. To clarify, this difference refers to the amount of CO_2 absorbed in the 50 % mixture during the first cycle (49 $g_{CO_2}/kg_{solution}$), minus the amount absorbed in the 25 % mixture (34 $g_{CO_2}/kg_{solution}$) or the 12.5 % mixture (18.7 $g_{CO_2}/kg_{solution}$) in the first cycle. Similarly, in the second and third cycle, the difference is calculated by subtracting the amount absorbed in the 25 % mixture (21.3–20.5 $g_{CO_2}/kg_{solution}$) or the 12.5 % mixture (11.3–10.3 $g_{CO_2}/kg_{solution}$) from the amount absorbed in the 50 % mixture (28–27 $g_{CO_2}/kg_{solution}$). On the right axis, the regeneration efficiency is illustrated. As mentioned above, the operating conditions are not favourable for a MEA solution. As a result, the regeneration efficiency at the second and third cycle is very low and <10 %. For all the mixtures, a regeneration efficiency higher than 55 % is achieved in the second cycle and remains stable in the last. Several studies have documented limitations in absorption efficiency during CO_2 capture processes utilizing ILs. Reference [19] reported a decrease in regeneration efficiency after five cycles for three different solutions (H_2NCH_2COONa, MEA, and [C_2OHmim][Gly]), ranging from 7 % to 17 % loss, in a 250 ml stirred double cell reactor operating at over 100 °C. This highlights the potential for degradation over time, even under controlled laboratory conditions. Furthermore, authors [20] observed a significant reduction in capture efficiency (up to 70 %) for

Table 5
CO_2 absorbed and desorbed at each cycle in terms of moles.

Solution	Cycle	CO_2 absorbed [mol]	CO_2 desorbed [mol]
12.5 %	1	0.23	0.11
	2	0.14	0.1
	3	0.13	0.09
25 %	1	0.77	0.34
	2	0.48	0.40
	3	0.46	0.33
50 %	1	1.15	0.69
	2	0.66	0.55
	3	0.63	0.63
30 % MEA	1	1	0.31
	2	0.09	0.24
	3	0.07	0.24

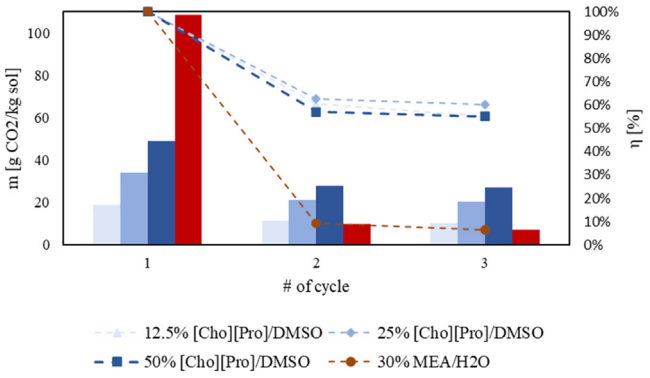

Fig. 7. Cyclic CO_2 absorption measurements over 3 absorption/desorption cycles. The left axis refers to the bar graphs reporting the mass CO_2 absorption loading. The right axis refers to the regeneration efficiency.

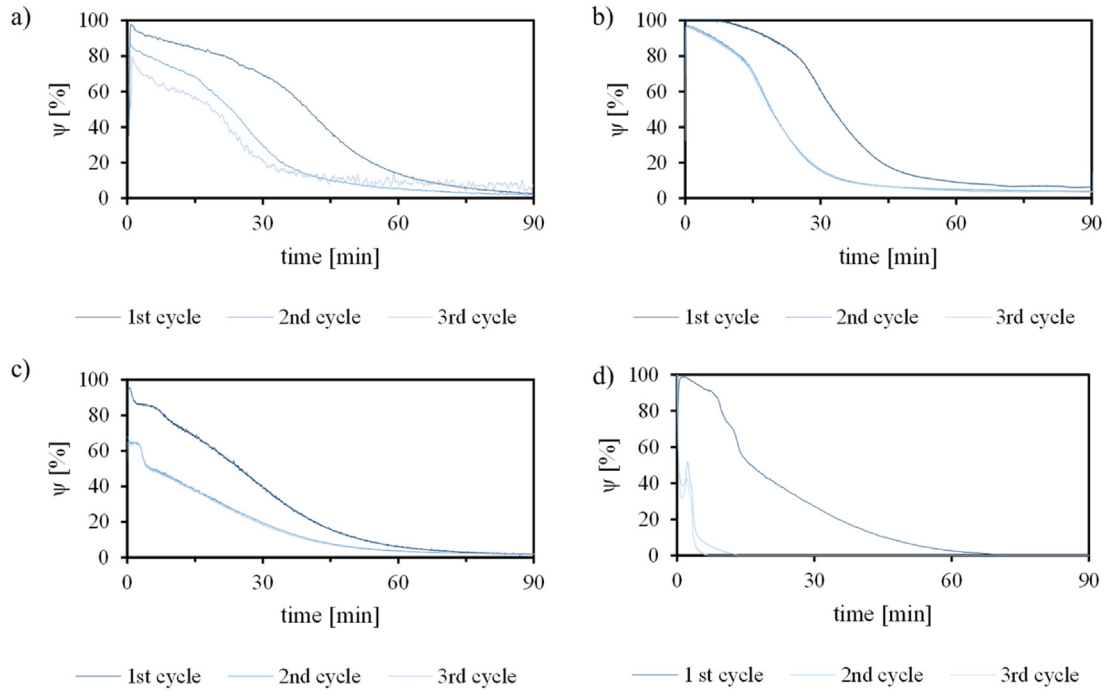

Fig. 8. CO_2 removal rate for three consecutive cycles: a)12.5 % wt [Cho][Pro] in DMSO (30 second moving average); b) 25 % wt [Cho][Pro] in DMSO; c) 50 % wt [Cho][Pro] in DMSO; d) 30 % wt MEA in H2O.

an IL sample as small as 2 g, measured using a gravimetric balance. This rapid decline, even with minimal sample quantities, suggests inherent limitations within certain ILs or potential degradation mechanisms during the capture process.

The initial test results indicate that the solutions tend to stabilize from the third cycle onward. Furthermore, the solution with an intermediate concentration demonstrates intermediate performance in terms of both molar and mass CO_2 absorption.

The CO_2 removal rate is an important parameter to evaluate because it quantifies the efficiency and effectiveness of the CO_2 capture solution in terms of its ability to reduce carbon dioxide emissions and mitigate climate change. Evaluating the CO_2 removal rate is crucial for several reasons. Firstly, it helps assess the feasibility and viability of a CO_2 capture process. A high removal rate indicates that a significant amount of CO_2 is being captured, making the process more effective in reducing greenhouse gas emissions. The CO_2 removal rate directly impacts the cost-effectiveness of the process. Higher removal rates often result in lower operational costs per unit of CO_2 captured, making the technology more economically attractive. On the other hand, a low removal rate may suggest the need for improvements or reduce the ratio between the CO_2 flow rate that enters in the reactor over the mole of IL in the absorption column.

The incomplete regeneration observed in this study can be attributed to the conditions under which regeneration is conducted. Unlike controlled laboratory environments, where the volume is reduced and external factors such as hydrostatic pressure is practically absent, the real-world setup introduces additional complexities. Specifically, the pressure exerted by the liquid column in the regeneration system creates a backpressure that may inhibit the complete desorption of CO_2. This pressure prevents the CO_2 from fully escaping the liquid phase, leading to less effective regeneration. In laboratory conditions complete desorption is often achievable [14]. However, in practical applications, this is more challenging due to the continuous operational conditions and the need to balance system pressure.

Fig. 8 presents the results obtained for each of the proposed solutions at different numbers of cycles. All initial mixtures exhibit high CO_2 removal rate, exceeding 90 % in the first few minutes. However, in subsequent cycles, both the 12.5 % IL and the 50 % IL mixtures cannot achieve the desired target. The limited performance of the 12.5 % IL mixture can be attributed to its lower concentration, which slows down the interaction between CO_2 and the liquid ion molecules. Conversely, the high viscosity of the 50 % IL mixture hinders effective bonding between the reactants, leading to reduced CO_2 capture.

The 25 % wt [Cho][Pro] blend is the most effective among the tested compositions. Nevertheless, even this mixture fails to capture 90 % of CO_2 within the first 10 min of absorption. These findings suggest that the solution with an intermediate composition performs better in this case, indicating the need for a detailed investigation into the ratio of CO_2 flow rate to molar IL. Further analysis and optimization of this parameter will be necessary to enhance the overall performance of the CO_2 capture system.

3.3.2. *Effect of temperature*

The subsequent investigation focused on examining the influence of temperature on the absorption and desorption processes after completing the three cycles, as discussed earlier. Similarly to the cyclability test, the same ionic liquid solutions were introduced into the reactor and heated to the desired operating temperature. Isothermal absorption tests were conducted at 30 °C, 40 °C, and 50 °C, with a constant flow rate of 30 $\frac{Nl}{h}/mol_{IL}$ of CO_2 for 90 min, as shown in Fig. 9 on the left side. Following each absorption at the designated temperature, the solution was cooled to 30 °C and saturated with CO_2 for 30 min (i.e., illustrated in the middle side of the figure). The regeneration process involved incrementally raising the reactor temperature to 70 °C for 60 min, 80 °C, and 90 °C, maintaining both temperatures (80 °C and 90 °C) for 30 min. A summary of the experimental procedures is provided in Fig. 9.

Fig. 10 illustrates the CO_2 absorption process at 30 °C for all three solutions, followed by saturation and regeneration. Notably, the reactor's temperature remained stable at 30 °C during the absorption test with the 12.5 % wt [Cho][Pro] mixture, eliminating the need for a satura-

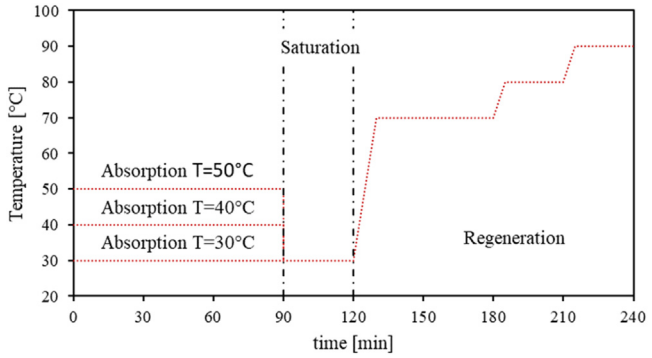

Fig. 9. Temperature evolution scheme. On the first side, an absorption test at different temperatures is performed, then the reactor is cooled at 30 °C and the solution is saturated. Finally, a regeneration test at different temperature steps is performed.

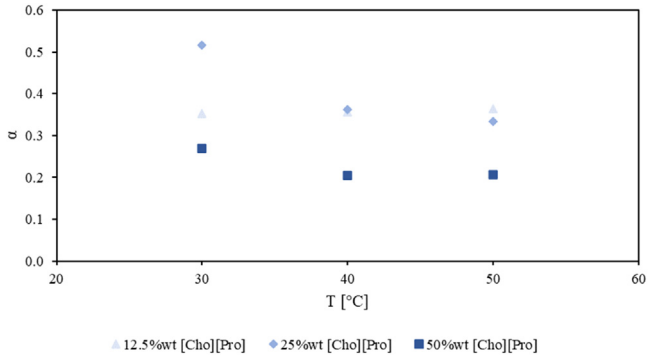

Fig. 11. Temperature effect on the absorption test.

tion phase. This result indicates effective absorption without additional temperature regulation and demonstrates the low exothermicity of the reaction. Fig. 10 demonstrates the significant impact of regeneration temperature on the CO_2 desorption process. The 50 % wt [Cho][Pro] solution alone can achieve complete regeneration at 80 °C, aligning with Fig. 6's findings. In contrast, the other two mixtures exhibit incomplete regeneration. Each increase in temperature brings a noticeable shift in the alpha trend, marking an instant CO_2 release before entering a stabilization phase.

Fig. 11 shows the final molar CO_2 absorption loading for each solution at three different absorption temperatures, highlighting the measurements taken before reaching saturation at 30 °C. It is evident that as the absorption temperature rises, the alpha value decreases (except for the 12.5 % mixture that shows remarkable stability). The operating absorption temperature impacts the capacity loading, with higher amounts of carbon dioxide being absorbed at lower temperatures. This finding can be attributed to the exothermic nature of the absorption reaction when using ILs as carbon capture solvents. These tests reaffirm that the 25 % wt [Cho][Pro] solution consistently outperforms the others even at higher temperatures, except 50 °C where the 12.5 % wt IL mixture exhibits a slightly higher value.

3.4. Long-term stability test

Assessing a solution's performance stability across multiple CO_2 capture cycles is crucial for long-term effectiveness and reliability. This analysis reveals the solution's behaviour over time, highlighting its sustainability and practical application durability. Moreover, it identifies any efficiency losses or degradation, crucial for addressing issues that might affect performance. Stability assessments are also key for process optimization and scaling, ensuring the solution's ongoing effectiveness in capturing CO_2. If a solution exhibits consistent and stable performance over multiple cycles, it instils confidence in its reliability and suitability for large-scale CO_2 capture applications. This information can guide decision-making processes, such as selecting the most effective solution and determining the optimal operational conditions.

Among the three solutions tested, only one was selected for extended performance evaluation over a high number of cycles, due to the considerable time required for each cycle (approximately one cycle per day). To determine the most suitable solution for this extended study, the performance of the three solutions was compared during their third cycle. The indicators used for comparison were molar absorption (α), absorption capacity (m), regeneration efficiency (η), and the CO_2 removal rate after 5 min from the start of the third absorption cycle (ψ). Additionally, molar absorption at 50 °C was also considered. The results of this comparison are presented in Fig. 12.

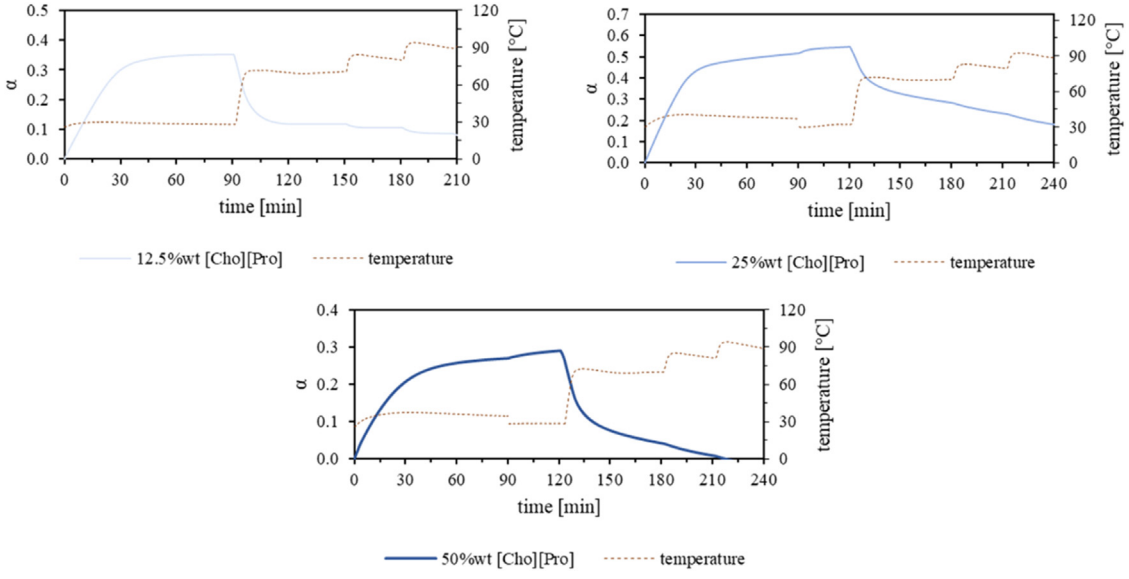

Fig. 10. Molar efficiency evolution during the absorption step performed at 30 °C, saturation step, and regeneration step.

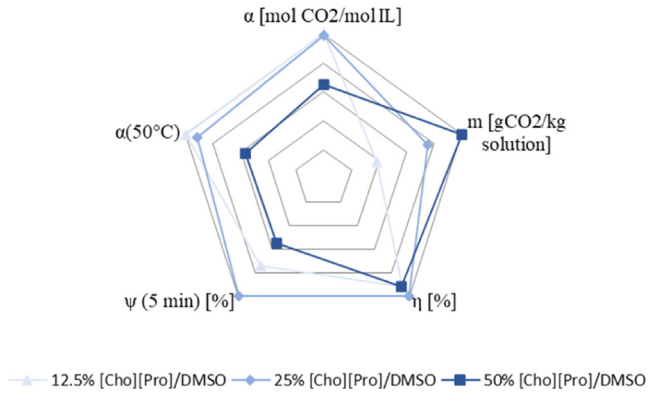

Fig. 12. Comparison of the indicators chosen for the three solutions with different compositions.

The solution containing 25 % wt of [Cho][Pro] in DMSO demonstrated good performance in all the key indicators. In the third cycle, the solution achieved a CO_2 removal rate (after 5 min) exceeding 90 %, significantly outperforming the other mixtures, which recorded 67 % and 49.5 % for the 12.5 % IL and 50 % IL solutions, respectively. This performance aligns with the technical requirement of removing >90 % of CO_2 from the incoming fumes. However, its absorption capacity is slightly lower, reaching 20.5 g CO_2/kg solution compared to 27 g CO_2/kg solution for the 50 % [Cho][Pro] mixture. Despite this, the 25 % IL mixture outperforms the 50 % IL mixture in all four other key indicators, making it the ideal choice for further experimental testing. Based on these findings, a new blank solution was prepared (i.e., 0.9974 kg loaded in the reactor) and subjected to 30 cycles of absorption at 30 °C and desorption at 80 °C, following the same conditions as the cycling test described earlier. Fig. 13 clearly illustrates that the regeneration efficiency experiences a significant drop after the first cycle. However, it stabilizes at around 55 % and maintains this value consistently throughout the subsequent 30 cycles. This result indicates that while the mixture may not achieve complete regeneration under the given conditions, it does not undergo degradation over repeated cycles.

Fig. 14 provides a detailed analysis of the molar CO_2 absorption loading and CO_2 removal rate for cycles 1, 10, 20, and 30. The data indicates that the solution's performance is significantly better in the first cycle than in later cycles. However, it is noteworthy that cycles 10, 20, and 30 exhibit nearly identical absorption characteristics, indicating exceptional stability of the material over time. The similarity in absorption performance between cycles 10, 20, and 30 suggests that the material reaches a state of equilibrium after the initial cycle, wherein its performance remains consistent and reliable throughout subsequent cycles.

Unlike traditional amine-based solvents like MEAs, there is no requirement to replace or supplement the solution in the reactor. Its consistent performance over multiple cycles ensures its suitability for prolonged use in CO_2 capture applications without frequent changes or additional interventions. This characteristic enhances the overall viability and cost-effectiveness of the solution, contributing to its practical applicability and environmental impact.

Solution stabilities were assessed using ATR spectroscopy to verify the preservation of their structures without noticeable degradation. For the sake of concision only the comparison between the 25 % wt solution before and after testing was performed, it's important to note that similar outcomes were observed across all solutions tested.

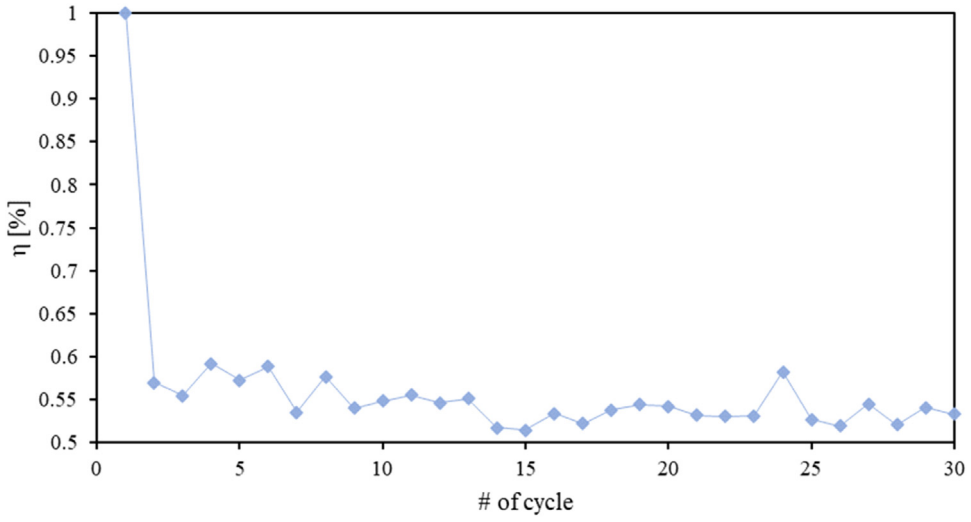

Fig. 13. Long-term stability test on the solution composed of 25 % wt [Cho][Pro] in DMSO.

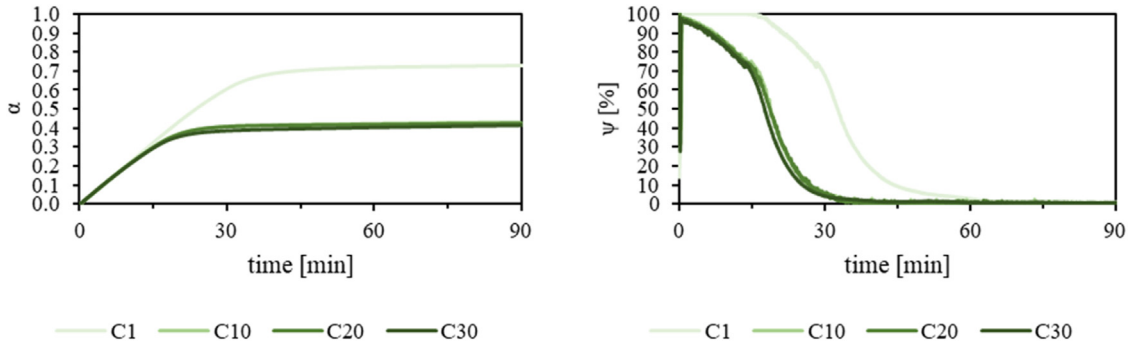

Fig. 14. Molar CO_2 absorption loading (on the left) and CO_2 removal rate (on the right) resulted from cycles 1, 10, 20 and 30.

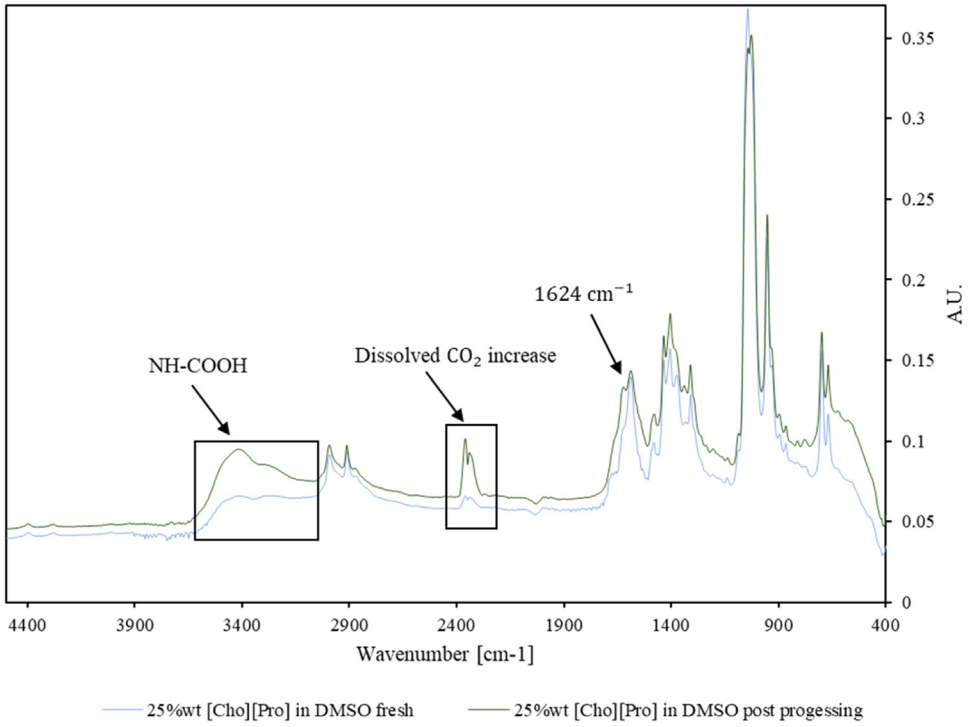

Fig. 15. ATR spectroscopic analysis of [Cho][Pro]-DMSO 25wt % solution before and after absorption cycles. Physical CO_2 retention in DMSO (around 2250 cm^{-1}), chemically bound carbamate -NH_2^+ at 1624 cm^{-1} and carbamate acid -OH stretching (3600–3000 cm^{-1}).

In the case of the [Cho][Pro]-DMSO 25 wt % solution (see Fig. 15), the ATR spectra show slight modifications after all absorption cycles. Notably, the spectra demonstrate the retention of CO_2, both physically dissolved in DMSO (evident around 2250 cm^{-1}) and chemically bound in the carbamate form. The formation of CO_2 is further corroborated by the protonation of the secondary amine, leading to the creation of NH_2^+ species, a result of ammonium carbamate formation. The asymmetric NH_2^+ bending modes are discernible at 1624 cm^{-1}. Additionally, the formation of carbamate acid is indicated by the enhanced -OH stretching observed in the range of 3600 to 3000 cm-1. This detailed analysis aligns with findings by G. Latini et al. [12] in their study on the CO_2 reaction mechanism in bio-based amino-acid ionic liquids, as revealed through operando ATR-IR spectroscopy. Importantly, the spectral analysis provides no evidence of degradation for either the ionic liquid (IL) or DMSO, indicating the solutions' stability under the tested conditions.

4. Conclusion and perspectives

In conclusion, our comprehensive investigation aimed to characterize and evaluate the performance of different solutions containing [Cho][Pro] in DMSO for CO_2 capture processes. Through a series of experimental tests and analyses, we examined various aspects of the absorption and desorption processes, including the influence of temperature, concentration, and cycling on CO_2 capture and release. A key finding is the existence of an optimal IL concentration that balances viscosity and reactivity, significantly influencing CO_2 capture efficiency. Specifically, the 25 % wt [Cho][Pro] solution demonstrates that an intermediate concentration provides sufficient reactive sites while maintaining low enough viscosity to facilitate effective mass transfer. This optimal balance results in superior CO_2 uptake, surpassing 90 % absorption, and excellent regeneration efficiency over multiple cycles exhibiting remarkable stability and durability with absorption and desorption performance remaining nearly identical from the 10th to the 30th cycle. The performance of IL-based CO_2 capture systems is maximized when the concentration achieves an optimal balance between chemical reactivity and physical mass transfer properties. Excessively high concentrations increase viscosity, hindering diffusion, while too low concentrations lack sufficient reactive sites for effective CO_2 capture. However, it is important to recognize that viscosity increases during CO_2 capture due to the formation of carbamic acid and ammonium-carbamate, which can affect mass transfer rates and overall process efficiency. Therefore, future studies should evaluate the changes in viscosity during and after CO_2 absorption. Understanding how viscosity evolves throughout the capture and release cycles will be crucial for optimizing IL formulations and operational parameters. Moreover, the use of a high-boiling diluent like DMSO emerges as a general strategy to mitigate viscosity issues inherent in ILs, enhancing mass transfer without diminishing too much the chemical absorption capacity. This approach underscores the broader applicability of diluents in designing efficient CO_2 capture solvents. Looking ahead, optimizing operating conditions such as temperature and IL concentration can further enhance performance, potentially leading to complete regeneration of the solution. Assessing scalability and economic viability remains crucial for their practical adoption in large-scale industrial application.

Declaration of competing interest

The authors declare that they have no known competing financial interests or personal relationships that could have appeared to influence the work reported in this paper.

CRediT authorship contribution statement

Salvatore F. Cannone: Writing – review & editing, Writing – original draft, Visualization, Software, Methodology, Investigation, Data curation, Conceptualization. **Michel Tawil:** Writing – review & editing, Software, Methodology, Investigation. **Sergio Bocchini:** Writing – review & editing, Writing – original draft, Supervision, Methodology, Funding acquisition, Conceptualization. **Massimo Santarelli:** Writing – review & editing, Supervision, Conceptualization.

Acknowledgments

This study was carried out within the Agritech National Research Center and received funding from the European Union Next-

GenerationEU (PIANO NAZIONALE DI RIPRESA E RESILIENZA (PNRR) – MISSIONE 4 COMPONENTE 2, INVESTIMENTO 1.4 – D.D. 1032 17/06/2022, CN00000022). This manuscript reflects only the authors' views and opinions, neither the European Union nor the European Commission can be considered responsible for them.

This article was partially funded under the National Recovery and Resilience Plan (NRRP), Mission 4 "Education and Research"—Component 2 "From research to business"—Investment 3.1 "Fund for the realization of an integrated system of research and innovation infrastructures"—Call for tender No n. 3264 of 28/12/2021 of Italian Ministry of Research funded by the European Union—NextGenerationEU—Project code: IR0000027, Concession Decree No 128 of 21/06/2022 adopted by the Italian Ministry of Research, CUP: B33C22000710006, Project title: iENTRANCE.

Supplementary materials

Supplementary material associated with this article can be found, in the online version, at doi:10.1016/j.ccst.2024.100312.

References

Wei, Y.M., et al., Feb. 2021. A proposed global layout of carbon capture and storage in line with a 2 °C climate target. Nat Clim Chang 11 (2), 112–118. doi:10.1038/s41558-020-00960-0.

Bocchini, S., et al., 2017. The Virtuous CO $_2$ Circle or the Three Cs: Capture, Cache, and Convert. J Nanomater 2017, 1–14. doi:10.1155/2017/6594151.

Cannone, S.F., Lanzini, A., Santarelli, M., 2021. A Review on CO2 Capture Technologies with Focus on CO2-Enhanced Methane Recovery from Hydrates. Energies (Basel) 14 (2). doi:10.3390/en14020387.

Chao, C., Deng, Y., Dewil, R., Baeyens, J., Fan, X., Mar. 2021. Post-combustion carbon capture. Renewable and Sustainable Energy Reviews 138, 110490. doi:10.1016/j.rser.2020.110490.

Bernhardsen, I.M., Knuutila, H.K., Jun. 2017. A review of potential amine solvents for CO 2 absorption process: Absorption capacity, cyclic capacity and pKa. International Journal of Greenhouse Gas Control 61, 27–48. doi:10.1016/j.ijggc.2017.03.021.

Nasirpour, N., Mohammadpourfard, M., Heris, S.Zeinali, Aug. 2020. Ionic liquids: Promising compounds for sustainable chemical processes and applications. Chemical Engineering Research and Design 160, 264–300. doi:10.1016/j.cherd.2020.06.006.

Zhao, H., Baker, G.A., Jan. 2023. Functionalized ionic liquids for CO $_2$ capture under ambient pressure. Green Chem Lett Rev 16 (1). doi:10.1080/17518253.2022.2149280.

Aghaie, M., Rezaei, N., Zendehboudi, S., Nov. 2018. A systematic review on CO2 capture with ionic liquids: Current status and future prospects. Renewable and Sustainable Energy Reviews 96, 502–525. doi:10.1016/j.rser.2018.07.004.

Nematollahi, M.H., Carvalho, P.J., Aug. 2019. Green solvents for CO2 capture. Curr Opin Green Sustain Chem 18, 25–30. doi:10.1016/j.cogsc.2018.11.012.

Hua, L., Jun. 2009. Thermodynamic model of solubility for CO $_2$ in dimethyl sulfoxide. Phys Chem Liquids 47 (3), 296–301. doi:10.1080/00319100701788360.

Shokouhi, M., Farahani, H., Hosseini-Jenab, M., Apr. 2014. Experimental solubility of hydrogen sulfide and carbon dioxide in dimethylformamide and dimethylsulfoxide. Fluid Phase Equilib 367, 29–37. doi:10.1016/j.fluid.2014.01.020.

Latini, G., Signorile, M., Crocellà, V., Bocchini, S., Pirri, C.F., Bordiga, S., 2019. Unraveling the CO2 reaction mechanism in bio-based amino-acid ionic liquids by operando ATR-IR spectroscopy. Catal Today 336, 148–160. doi:10.1016/j.cattod.2018.12.050.

Davarpanah, E., Hernández, S., Latini, G., Pirri, C.F., Bocchini, S., 2020. Enhanced CO2 Absorption in Organic Solutions of Biobased Ionic Liquids. Adv Sustain Syst 4 (1), 1900067. doi:10.1002/adsu.201900067.

Latini, G., et al., 2022. Efficient and reversible CO2 capture in bio-based ionic liquids solutions. Journal of CO2 Utilization 55, 101815. doi:10.1016/j.jcou.2021.101815.

Meng, F., Meng, Y., Ju, T., Han, S., Lin, L., Jiang, J., Oct. 2022. Research progress of aqueous amine solution for CO2 capture: A review. Renewable and Sustainable Energy Reviews 168, 112902. doi:10.1016/j.rser.2022.112902.

Barzagli, F., Mani, F., Peruzzini, M., Jul. 2016. A Comparative Study of the CO2 Absorption in Some Solvent-Free Alkanolamines and in Aqueous Monoethanolamine (MEA). Environ Sci Technol 50 (13), 7239–7246. doi:10.1021/acs.est.6b00150.

Latini, G., Signorile, M., Crocellà, V., Bocchini, S., Pirri, C.F., Bordiga, S., Oct. 2019. Unraveling the CO2 reaction mechanism in bio-based amino-acid ionic liquids by operando ATR-IR spectroscopy. Catal Today 336, 148–160. doi:10.1016/j.cattod.2018.12.050.

Hu, H., Li, F., Xia, Q., Li, X., Liao, L., Fan, M., Dec. 2014. Research on influencing factors and mechanism of CO2 absorption by poly-amino-based ionic liquids. International Journal of Greenhouse Gas Control 31, 33–40. doi:10.1016/j.ijggc.2014.09.021.

Lv, B., Xia, Y., Shi, Y., Liu, N., Li, W., Li, S., Mar. 2016. A novel hydrophilic amino acid ionic liquid [C2OHmim][Gly] as aqueous sorbent for CO2 capture. International Journal of Greenhouse Gas Control 46, 1–6. doi:10.1016/j.ijggc.2015.12.029.

Saravanamurugan, S., Kunov-Kruse, A.J., Fehrmann, R., Riisager, A., Mar. 2014. Amine-Functionalized Amino Acid-based Ionic Liquids as Efficient and High-Capacity Absorbents for CO $_2$. ChemSusChem 7 (3), 897–902. doi:10.1002/cssc.201300691.